Investigation of the elasticity of a cisplatin-DNA adduct via single-molecule measurements and bimodal modeling

Nam-Kyung Lee,[1,2,*] Jin-Sung Park,[3] Albert Johner,[2] Sergei Obukhov,[2,4] Ju-Yong Hyon,[5] Kyoung J. Lee,[3] and Seok-Cheol Hong[3,†]

[1]*Department of Physics, Institute of Fundamental Physics, Sejong University, Seoul 143-743, Korea*

[2]*Institut Charles Sadron, 670 83 Strasbourg Cedex, France*

[3]*Department of Physics, Korea University, Seoul 136-713, Korea*

[4]*Department of Physics, University of Florida, Gainesville, Florida 32611, USA*

[5]*Bio-microsystems Technology Program, Korea University, Seoul 136-713, Korea*

(Received 15 January 2009; published 22 April 2009)

Cisplatin has been known as an anticancer drug for a long time. It is therapeutically active upon binding to DNA. A double-bound cisplatin bends DNA into a localized kink. We model the elastic properties of cisplatin-DNA adducts at moderate tension (<6 pN). It is shown that from the mechanical point of view the action of cisplatin can be revealed by reduced persistence length. We derived two expressions for the persistence length, which apply in the linear-response and the strong-force regimes, respectively. Experimental data for DNA adducts stretched by magnetic tweezers are consistently fitted by these expressions. This allows us to estimate the degree of platination at various salt concentrations.

DOI: 10.1103/PhysRevE.79.041921 PACS number(s): 87.15.ad, 87.15.La, 87.14.gk, 87.80.Nj

I. INTRODUCTION

Cisplatin is among the earliest and best-known anticancer drugs [1]. It has been known for a long time that cisplatin functions by binding to DNA molecules [2]. The platination of DNA hinders DNA synthesis and interferes with its repair mechanism, eventually killing cells. Synthesis and testing of next-generation drug complexes constitutes a very active field of chemistry and medical science [3]. Thanks to Lippard and co-workers [4–6] and others [7–9], much is known about binding of cisplatin to DNA from the chemical and structural point of view [10]. Cisplatin is a planar complex $Pt(NH_3)_2(Cl)_2$, and the active form turns out not to be cisplatin itself but ionized hydrated forms, $Pt(NH_3)_2(H_2O)Cl^+$ and $Pt(NH_3)_2(H_2O)_2{}^{2+}$. The cationic complexes are favored over the neutral one in the vicinity of the negatively charged DNA. An excess of Cl^- anions can reverse the hydration and restore the inactive neutral form. The significance of this effect will be discussed later. Water is an easy-leaving group that can be further replaced, for example, by a nitrogen atom of DNA bases. Most important to our work are the intrastrand cross links between two neighboring guanine bases (GpG) which form nearly 68% of the adducts and are therefore responsible for altered mechanical properties under moderate force (~ 1 pN). Cisplatin binds to the N7's of two consecutive guanines, which are accessible from the major groove of DNA, resulting in a complex where a platinum atom is coordinated with four nitrogens. The platinated DNA has kinks at binding sites. From x-ray-diffraction [10], NMR [11], and gel-electrophoresis experiments [12,13], it is shown that a kink of GpG adduct bends the DNA helix by $\theta_k = 2\gamma = 40°$ and unwinds it by 13° upon cisplatin binding. As cisplatin mainly binds as $Pt(NH_3)_2{}^{2+}$, the chemical binding of these complexes onto negatively charged DNA backbone neutralizes the electrostatic charges around the kinks.

Although the electrostatic self-interaction stiffens DNA, such electrostatic interactions are screened out at high salt concentration and the intrinsic persistence (51 nm) applies to natural DNA. Our experiments were performed in the salt concentrations ranging from 10 to 160 mM, where we verified that the elasticity of bare DNA is well described by the intrinsic persistence length. In our study, we will neglect electrostatic stiffening throughout.

As cisplatin occupancy changes, the cisplatin-bound DNA undergoes a structural change due to the accumulation of kinks. We monitored such a structural change by measuring the force extension of cisplatin-DNA adducts using magnetic tweezers [14,15]. An external force is applied to one end of a double-stranded DNA (dsDNA) molecule while the other end is held fixed. Then the stretched DNA is incubated in the solution of cisplatin. In this way, DNA loops can be suppressed and cisplatin mainly binds at two consecutive GpG bases. As cisplatin binding continues under a constant force, the extension of DNA decreases due to the formation of kinks and the modified DNA is strengthened (more resilient against pulling).

For the last decades, single-molecule force spectroscopy measurements have revealed that the elastic response of a molecule reflects the internal structure of the molecule [16–18]. The earlier work by Krautbauer *et al.* [19] reported atomic force microscopy (AFM) experiments on cisplatin-bound DNA under large forces, especially focusing on the effect of intra- and interstrand cisplatin adducts on the B-S transition [the overstretching transition between the B- and S-form DNA] (~ 65 pN) and on the melting transition ($\sim 200-300$ pN) of DNA. It was shown that both transitions are far less cooperative than in the absence of cisplatin. Complementary experiments were performed on synthetic dsDNA of specific base sequences to attribute such mechanical changes to particular types of adducts.

*lee@sejong.ac.kr

†hongsc@korea.ac.kr

 ©2009 The American Physical Society

In this paper we consider a regime of much weaker forces (≤ 6 pN), well below the force for the B-S transition, typical of standard magnetic tweezers experiments [14]. Recently, we showed that the elasticity of a cisplatin-DNA adduct can be characterized by two separate persistence lengths at low- and high-tension regimes (yet below the B-S transition) and the degree of platination can be estimated via the bimodal modeling [15]. In this paper, we present a detailed theoretical description of the bimodal modeling which can be used to characterize the force-extension curves of cisplatin-DNA adducts at those moderate tensions and predict the cisplatin occupancy from the single-molecule experimental data. A short account of this work appeared in [15].

Double-bound cisplatin kinks a DNA molecule and modifies its elastic properties. Besides numerical studies on a single permanent kink by Li *et al.* [20], several analytical theories for DNA chains kinked by bound chemicals or proteins have been provided in recent years. Wiggins *et al.* [21] considered annealed kinks with a variable kink angle. Popov and Tkachenko [22] studied kinks with a fixed kink angle induced by chemicals in full equilibrium with the embedding solution. Kulic *et al.* [23] provided a theory for DNA elasticity where kinks are produced by sliding loops. In these cases, the persistence length under high tension recovers that of bare DNA. There is, however, no evidence for unbinding of cisplatin (or kink angle flattening) in our experiments. As also mentioned in Ref. [4], double-bound cisplatin is unable to desorb or to efficiently move along DNA during the measurement. Thus, it is necessary to develop a theory to handle our situation where quenched kinks are located along the DNA backbone. In order to model the influence of irreversible kinks on DNA elasticity, we distinguish two limiting cases depending on the magnitude of the external force.

As we stay well below the B-S transition of DNA molecules, dsDNA can be characterized by its stiffness only and hence modeled as, otherwise featureless, wormlike chain. All microscopic details go into one unique parameter, the persistence length l_p, which characterizes the decay of orientational correlation along the chain [24]. Qualitatively, such a chain can be viewed as rigid at scales smaller than the persistence length l_p and flexible (fluctuating) at larger scales. The correlation in the orientation of the tangent vector $\mathbf{u}$ decays exponentially along the contour over the persistence length l_p due to thermal fluctuations, $\langle \mathbf{u}(s)\cdot\mathbf{u}(s')\rangle = \exp(-|s-s'|/l_p)$, with s as the curvilinear coordinate along the chain. Bending the chain locally with a curvature C costs an elastic energy of $k_B T l_p C^2/2$ per unit length. Summing up the orientational correlations yields the average end-to-end distance $\langle R^2\rangle_0 = 2Ll_p$ of a free chain where the contour length L is assumed to be much larger than l_p. (In fact, the DNA used in our experiments is a few micrometers long, which is about 2 orders of magnitude longer than the intrinsic persistence length $l_p = 51$ nm, relevant here, of DNA.) Under a "diverging" force, the chain stretches out completely and $R^2 = x^2 = L^2$, with x as the extension along the direction of the force. Under a large but finite force $f \gg k_B T/l_p$, x is shortened due to transverse fluctuations $L - \langle x\rangle = \frac{L}{2}\sqrt{\frac{k_B T}{f l_p}}$. The force-extension curve is described by the widely used interpolation formula [25–27]

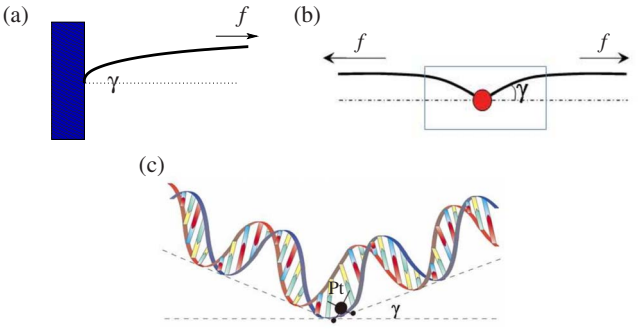

FIG. 1. (Color online) (a) Stiff chain under an external force f with the imposed boundary angle γ. (b) Illustration of a part of the kinked chain with the half-kink angle $\gamma = \theta_k/2$. (c) Illustration of cisplatin binding on DNA.

$$\frac{f l_p}{k_B T} = \frac{x}{L} + \frac{1}{4(1 - x/L)^2} - \frac{1}{4}. \tag{1}$$

In the linear-response regime ($x/L \ll 1$), Eq. (1) takes the form $x = \frac{\langle x^2\rangle_0}{k_B T} f$, with $\langle x^2\rangle_0 = \langle R^2\rangle_0/3$. At large force, the aforementioned asymptotic behavior, $L - x = \frac{L}{2}\sqrt{\frac{k_B T}{f l_p}}$, is recovered. For DNA, this asymptotic behavior applies at forces well below the ones required for any structural transition. Equation (1) is a convenient and satisfactory interpolation between the linear response and the full stretching, asymptotic response.

Imposing a single kink on a (locally) rigid chain amounts to imposing a (rather) small angle $\gamma \approx 20°$ between the strand and the direction of force at the kink (see Fig. 1). The external stretching force introduces an extra correlation length as discussed below. The angle has to relax, bringing the strand back parallel to the direction of force at the expense of the bending energy. Equating the typical bending energy $k_B T l_p (\gamma/\Lambda)^2 \Lambda$ to the work against the tension $f\gamma^2\Lambda$, it is easy to show that the relaxation length of the kink angle is $\Lambda = \sqrt{k_B T l_p / f}$ under a given force f. For forces larger than $k_B T/l_p$, Λ is smaller than l_p and thus relevant; otherwise the correlation length is just l_p. From the formal point of view, kinks are always uncorrelated at the tension large enough to make Λ smaller than their separation, in which case kinks can be treated separately.

There are two contributions to the elastic response under the high tension ($f \gg k_B T/l_p$): one corresponds to ironing-out of fluctuations and the other to extracting the stored length from the kinked regions. Both scale as $\sim -1/\sqrt{f}$. We will define the effective persistence length reflecting both contributions in Sec. II A.

If the applied force is small ($f \ll k_B T/l_p$), the orientations of kinks are not necessarily aligned along the direction of the external force. As the kinked sites (such as consecutive G's) are *randomly* distributed along the chain, the large-scale chain orientation can be treated as a random walk with various step sizes ("random-flight model"). We consider this regime in Sec. II B.

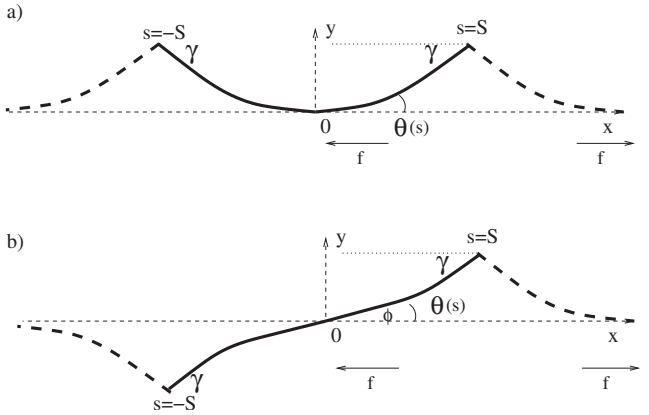

FIG. 2. Symmetric and skew-symmetric configurations. The origin is chosen to be the middle point between two neighboring kinks. At the boundary of subchain, $s=\pm S$, the angle γ is imposed at kink.

II. ELASTICITY OF A KINKED FILAMENT

A. Large-force limit

A semiflexible chain is described by position $\mathbf{r}(s)$ at a curvilinear coordinate s along the chain. The tangent vector is $\mathbf{u}(s) \equiv \partial \mathbf{r}(s)/\partial s$ with the constraint of $\mathbf{u}^2(s)=1$ for all s. The energy of a stiff filament consists of the bending energy and the external force contributions,

$$\frac{E}{k_B T} = \frac{l_p}{2}\int_{-S}^{S} ds \left(\frac{d\mathbf{u}(s)}{ds}\right)^2 - \frac{\mathbf{f}}{k_B T}\cdot[\mathbf{r}(L)-\mathbf{r}(0)], \qquad (2)$$

where the applied force is coupled to the end-to-end extension $x=\hat{x}\cdot[\mathbf{r}(L)-\mathbf{r}(0)]$ with $\hat{x}$ in the direction of the force (see Fig. 2). In the following we stick to the planar case for the sake of simplicity. The Lagrangian can be set as

$$L = \int ds \left[\frac{l_p k_B T}{2}\left(\frac{d\theta(s)}{ds}\right)^2 - f\cos\,\theta(s)\right], \qquad (3)$$

where $\theta(s)$ is the angle between the tangential vector and the x axis at the curvilinear coordinate s and f is the external force. The optimal shape obeys the following Euler equation:

$$l_p k_B T \frac{d^2\theta}{ds^2} - f\sin\,\theta(s) = 0. \qquad (4)$$

1. Isolated kink on a rigid chain

We first evaluate the characteristic relaxation length Λ of the kink angle under the given external force f. When the orientation of one end of the formally infinite filament is imposed with a certain angle γ at $s=0$ (see Fig. 1), the equation of motion [Eq. (4)] can be integrated with the boundary condition $\theta(s)\to 0$ when $s\to\infty$, to obtain the optimal shape:

$$\tan[\theta(s)/4] = \tan(\gamma/4)\exp(-s/\Lambda), \quad \Lambda = \sqrt{k_B T l_p/f}, \qquad (5)$$

with the expected correlation length Λ. If $\gamma/4$ remains small, we can approximate $\tan[\theta(s)/4]\approx\theta(s)/4$ and obtain $\theta(s)=\gamma\exp(-s/\Lambda)$. The optimal shape for the actual kink angle γ is sketched in Fig. 2. Integrating $1-\cos\,\theta(s)$ along the strand gives the end-to-end distance variation due to the length stored in the kink, $L-x=8\Lambda\sin^2(\gamma/4)$. The free-energy cost for imposing the kink is $16f\Lambda\sin^2(\gamma/4)$ or $f\Lambda\gamma^2$ after expansion. The linearized expression generally applies. If we insert typical numbers ($f=1$ pN, $l_p=51$ nm), a stored length of ~ 1 nm, a correlation length $\Lambda\sim 15$ nm, and a kink energy of ~ 1 kJ/mol or $0.4k_BT$/kink come out. This accounts for the large-scale deformation. We should keep in mind that adducts also locally perturb the double-helix structure, which leads to energy contributions of similar magnitude [5] (the core energy of a kink defect). Note that for monovalent salt concentration of 10 mM, the Debye screening length is about 3 nm, which is smaller than Λ. Thus neglecting the electrostatic interactions seems to be a valid approximation.

2. Extension of symmetric and skew-symmetric conformations

If the position of guanine is random, the typical distance between GpG shows an exponential distribution. We checked the correlation of guanine position of the DNA sequence which was used in the experiments and found that there is indeed no correlation. Nevertheless, we assume that the $f-x$ relation can be described as that for a typical contour length between kinks, $2S$. A DNA with multiple kinks can be modeled as a series of short interkink filaments whose boundary angles are imposed. Two kinks separated by less than the correlation length Λ are coupled, but two kinks separated more than Λ are independent. As an adduct bends the helix in the direction of the major groove, it would be, in principle, possible to change the azimuthal orientation of kinks in order to somewhat diminish the bending energy at the expense of torsional energy.

When kinks are close enough, reorienting them to reach a skew-symmetric configuration would significantly reduce the bending energy. However, the torsional persistence length l_t of DNA is typically twice as long as the bending persistence length [16]. Generically the torsional energy to invest in this reorientation is prohibitive. Thus, the azimuthal reorientation is not likely to happen. To estimate the free-energy difference and illustrate the uncoupling of neighboring kinks under high tension, we compare, for brevity, the cases of two planar configurations in which kinks are regularly spaced by $2S$: symmetric and skew-symmetric configurations as shown in Fig. 2. In fitting to experimental results, the uncoupled kink model that applies to high tension is used and these complications related to the azimuthal orientation are irrelevant. Angular deflections are all together small as illustrated by the study of an isolated kink.

As the angle θ remains small, we can approximate Eq. (4) to $l_p k_B T\frac{d^2\theta}{ds^2} - f\theta(s)=0$. The fixed angle at the kink $\gamma=\theta_k/2\approx 20°$ gives the boundary condition for symmetric/skew-symmetric conformation, indicated by the solid line in Fig. 2. The origin is taken at the midpoint between the two consecutive kinks of choice where $\theta(0)=0$ in the symmetric case and $\frac{d\theta}{ds}|_{s=0}=0$ in the skew-symmetric case. We describe the profile of one-half of the subchain. For a symmetric conformation, the solution is $\theta(s)=\frac{\gamma}{\sinh(S/\Lambda)}\sinh(s/\Lambda)$. For a skew-symmetric conformation, the solution is $\theta(s)=\frac{\gamma}{\cosh(S/\Lambda)}\cosh(s/\Lambda)$. Keeping the second order in θ, we ob-

tain the symmetric and skew-symmetric extensions X_S and X_A under a given force by integrating $1-\frac{1}{2}\theta^2(s)$ over a period $(4S)$,

$$X_S = 4S + \gamma^2 \frac{S}{\sinh^2(S/\Lambda)} - \frac{\Lambda\gamma^2}{2}\frac{\sinh(2S/\Lambda)}{\sinh^2(S/\Lambda)},$$

$$X_A = 4S - \gamma^2 \frac{S}{\cosh^2(S/\Lambda)} - \frac{\Lambda\gamma^2}{2}\frac{\sinh(2S/\Lambda)}{\cosh^2(S/\Lambda)}. \quad (6)$$

The free energies for a subchain of length $4S$ are

$$\sigma_S = 2\gamma^2 f\Lambda \coth\left(\frac{S}{\Lambda}\right),$$

$$\sigma_A = 2\gamma^2 f\Lambda \tanh\left(\frac{S}{\Lambda}\right), \quad (7)$$

which involve two kinks. The interaction between kinks is repulsive in the symmetric conformation and attractive in the skew-symmetric conformation. If the kink distribution would be annealed along DNA, kinks could be attractive to each other [22]. The energy gain per period (two kinks) by bringing two kinks closer, $|\sigma_A(S=0)-\sigma_A(S=\infty)|$, increases with the tension but is always at most of order k_BT in our experimental condition. Furthermore, in the large-force regime the attraction is also short ranged. As already mentioned, double-bound cisplatin can be considered as irreversibly bound on the time scale of the measurement. We do not expect any extra correlations between kinks to arise from this attraction. The free-energy difference is

$$\sigma_S - \sigma_A = 4\frac{k_BTl_p}{S}\gamma^2\frac{S}{\Lambda\sinh(2S/\Lambda)}. \quad (8)$$

For strongly coupled kinks $(S/\Lambda \to 0)$, the free-energy difference $\sigma_S-\sigma_A \sim 2k_BTl_p\gamma^2/S$, and for $\gamma=20°$ we expect the difference to be about $\frac{1}{4}\frac{l_p}{S}k_BT$, which can be as large as $\sim 10k_BT$. Our calculation shows that the skew-symmetric configuration has lower (bending) energy.

So far we considered a regular and infinite series of kinks with free (with respect to rotation) boundary conditions. In practice, the strand under consideration is finite and boundary conditions (for example, fixed twist angle) might control the ordering of the kinks. If there is no external torque applied at either end, the skew-symmetric configuration with all inflection points (including the ends) aligned along the external force is a minimum-energy solution. In order to convert a symmetric form to a skew-symmetric one, the subchain should twist by π over a contour length of $2S$. A typical energy cost due to twisting, $\pi^2\frac{l_t}{2S}k_BT$, is much larger than $\sigma_S-\sigma_A$ for $l_t > l_p$. Hence reorganization to all skew-symmetric sequences which would be naively anticipated from the two-dimensional (2-d) model does not take place. Only the full three-dimensional (3-d) model can consistently describe azimuthal correlations and torsional kinks. However, torsional effects of unwinding are not directly reflected by the force-extension curve [28]. There is no reason to investigate them thoroughly here.

For large force $(S/\Lambda \to \infty)$, $\sigma_S-\sigma_A \sim 8k_BT\frac{l_p\gamma^2}{\Lambda}e^{-2S/\Lambda}$. The difference vanishes exponentially as the external force increases. So does the difference in extension. This substantiates our previous argument that kinks become independent from each other under large force. Ultimately we recover the free-energy cost per isolated kink.

3. Ironing out thermal fluctuations

So far we have neglected thermal fluctuations. Neglecting the bending around kinks, we may calculate fluctuations as on a bare strand without adducts. This is justified at large tensions where the total length is not much affected by kinks. It is exact in the limit of small angular deviations relevant to our experiments. In this case it is enough to use the quadratic approximation in the deflection angle. We may still decompose the deflection in the Euler-Lagrange solution which carries the proper kink singularities and a deviation which is everywhere regularized by the bending energy (it is not necessarily a small correction to the Euler-Lagrange solution). It is then seen that the deviation obeys the usual free fluctuation calculation.

Let us recall the partition function of the fluctuations along a bare strand of length L in one transverse direction (normalized by its zero force value $\mathcal{Z}_{fl}^0$) [29]:

$$\frac{\mathcal{Z}_{fl}}{\mathcal{Z}_{fl}^0} = \sqrt{\frac{\pi\sqrt{\frac{f}{f_c}}}{\sinh\left(\pi\sqrt{\frac{f}{f_c}}\right)}}, \quad (9)$$

$$\mathcal{F}_{fl} - \mathcal{F}_{fl}^0 = \frac{k_BT}{2}\log\frac{\sinh\left(\pi\sqrt{\frac{f}{f_c}}\right)}{\pi\sqrt{\frac{f}{f_c}}}, \quad (10)$$

where $f_c = \pi^2 k_BTl_p/L^2$. The length stored in transverse fluctuations per each direction reads

$$\Delta L = -\frac{L^2}{4l_p}\left(\frac{\coth(L/\Lambda)}{L/\Lambda} - \frac{1}{L^2/\Lambda^2}\right). \quad (11)$$

For large force, the length stored in thermal fluctuations in both transverse directions (3-d strand) behaves asymptotically as

$$\Delta L = -\frac{L}{2}\sqrt{\frac{k_BT}{fl_p}} = -\frac{L\Lambda}{2l_p}. \quad (12)$$

On the other hand, the stored length by a kink under the same force [Eq. (6)] is

$$\Delta L = \frac{\gamma^2}{\sinh^2(S/\Lambda)}\frac{L}{4} - \frac{\Lambda L}{S}\frac{\gamma^2}{8}\frac{\sinh(2S/\Lambda)}{\sinh^2(S/\Lambda)} \underset{\Lambda\sim 00}{\to} -\frac{L}{2S}\frac{\gamma^2\Lambda}{2}. \quad (13)$$

The first term in the right-hand side is negligible in the limit of the strong force. Thus in the strong-stretching limit, we estimate the total extension as

$$x = L - \frac{L\Lambda}{2l_p} - \frac{L}{S}\frac{\gamma^2\Lambda}{4} \equiv L - \frac{L}{2}\sqrt{\frac{k_BT}{f}}\frac{1}{\sqrt{\Gamma^K}}, \tag{14}$$

where the last expression refers to a wormlike chain with the effective persistence length Γ^K:

$$\frac{1}{\sqrt{\Gamma^K}} = \frac{1}{\sqrt{l_p}}\left(1 + \gamma^2\frac{l_p}{2S}\right). \tag{15}$$

The force-extension curves shown in Fig. 3 obey Eq. (14) in the high-tension regime.

For example, if all G-G/C-C sites are occupied, we expect on average one kink per eight base pairs. There are $l_p/2S \sim 150/8$ kinks per l_p. By setting $\gamma = 20° \approx \pi/9$, we obtain the estimation of $\Gamma^K \approx 0.1l_p \approx 5$ nm (see Fig. 4, dashed line). In Sec. II B, we estimate the extension in the coil-like regime.

B. Linear-response regime

In the absence of external force, kinks due to cisplatin adducts deflect the chain configuration and effectively reduce the average coil size. The size R of a semiflexible chain is given by

$$R^2 = 2l_pL\left(1 - \frac{l_p}{L}(1 - e^{-L/l_p})\right). \tag{16}$$

In small-tension regime, the elasticity of the molecule is governed by the linear-response theory and the reduction in end-to-end fluctuation strengthens the molecule. The strengthening caused by kinking can thus be translated into an effective reduction of the persistence length. The corresponding physics is described by a random-flight model, which we modify here in order to take into account kinking effects.

Along the curvilinear length s, the correlation between tangent vectors decays as $\langle\cos\theta(s)\rangle = e^{-s/l_p}$. By a single kink, we assume that the tangent angle bends by θ_k within a base-pair distance a (=3.4 Å). Accordingly, we define s_k as the effective curvilinear length associated with θ_k,

$$\cos\theta_k = e^{-s_k/l_p}. \tag{17}$$

By inserting $\theta_k = 40°$ into Eq. (17), we obtain $s_k \approx 0.27l_p \approx 13.7$ nm. If a cisplatin binds to the backbone with the probability p, the tangent vector correlation in unit length ($\delta s = 1a$) can be described by

$$K \equiv \langle\cos\theta_1\rangle = (1-p)e^{-a/l_p} + pe^{-a/l_p - s_k/l_p}$$
$$= e^{-a/l_p}[1 - p(1 - e^{-s_k/l_p})]. \tag{18}$$

Two bond vectors $\mathbf{b}_n$ and $\mathbf{b}_{n+1}$, expressed on a unit sphere with the spherical coordinates (θ_n, ϕ_n) and $(\theta_{n+1}, \phi_{n+1})$, respectively, have an angle α between them: $\cos\alpha = \cos\theta_n\cos\theta_{n+1} + \sin\theta_n\sin\theta_{n+1}\cos(\phi_n - \phi_{n+1})$. Assuming that azimuthal angles are not correlated, the angular deviation of the bond vector m base pairs apart is $\langle\cos\theta_m\rangle = K^m$. For small $p \ll 1$, we can define the effective persistence length Γ^R as $\Gamma^R = -a/\ln(K)$. From the definition of s_k [Eq. (17)], we find the effective persistence length Γ^R for a cisplatin-bound DNA:

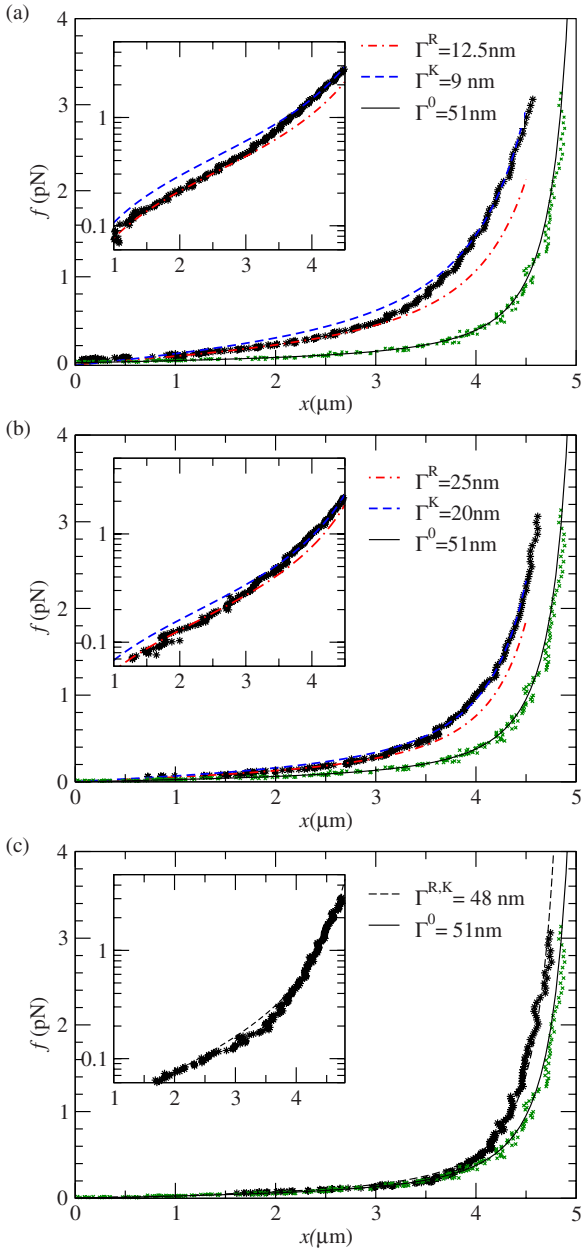

FIG. 3. (Color online) Force-extension data and their fits for DNA incubated in 3.3 mM cisplatin solution (a) with 20 mM salt, (b) with 60 mM salt, and (c) with 180 mM salt. The symbols represent experimental data and the lines are fits with an effective persistence length Γ. $\Gamma^K = 9$ nm for the large-force regime and $\Gamma^R = 12.5$ nm for the small-force regime in (a) and $\Gamma^K = 20$ nm ($\Gamma^R = 25$ nm) for the large-force (small-force) regime in (b). The inset of each panel shows the force-extension curves in semilogarithmic scale. The force extension of the natural DNA with 10 mM salt is also shown in both panels (rightmost curve) fitted with $\Gamma^0 = 51$ nm.

$$\frac{1}{\Gamma^R} = \frac{1}{l_p} + \frac{p}{a}(1 - e^{-s_k/l_p}). \tag{19}$$

Taking account of $p = 1/8$ in the saturation limit of cisplatin binding, we obtain $\Gamma^R \approx 27.8a \approx 9.5$ nm. It is 18.6% of the persistence length of bare dsDNA. Hence, the coil size of

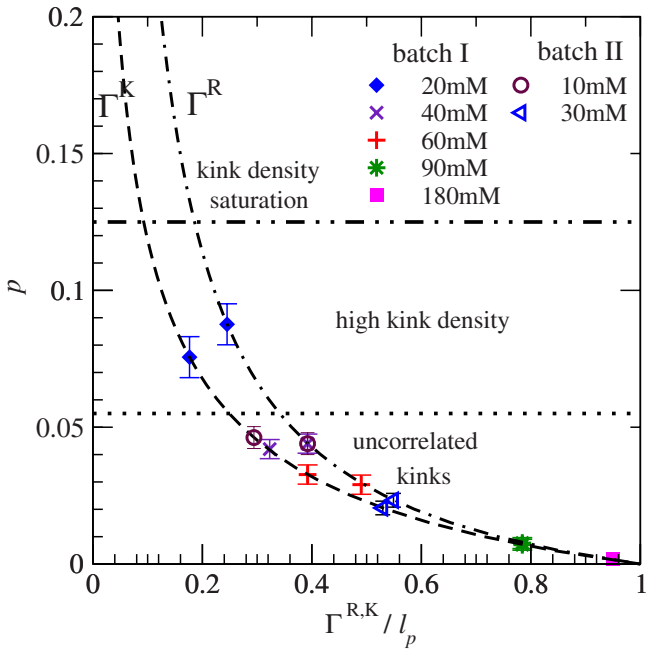

FIG. 4. (Color online) The effective persistence lengths $\Gamma^{K,R}/l_p$ vs the degree of cisplatin binding. The dot-dashed line is from the random-flight model suitable for the low-tension regime and the dashed line is from the aligned-kink model for the high-tension regime. From each force-extension measurement, we extract the effective l_p by fitting the curves with Eq. (20). By comparing the experimental values with the two theoretical expressions of the effective l_p (i.e., Γ^R,Γ^K), we obtained a pair of p values. We also show error bars in the estimate of p. The size of error bar indicates the standard deviation of p values from different measurements. Symbols represent the experimental data under various conditions. The maximum concentration for a random sequence is expected to be around $p=1/8=0.125$, limited by inherent G-G pairs. We used $l_p/a=150$ for fitting.

the platinated DNA can be estimated by replacing l_p with Γ^R in Eq. (16) at the maximum loading. The DNA coil size thus decreases as more and more kinks are formed. The relative change in coil size $R^2(p)/R^2(0)$ at cisplatin occupancy p is $\sim\Gamma^R/l_p$.

For a semiflexible chain carrying $n=p(L/a)$ kinks, the force-extension relation in the small-force regime ($l_p<\Lambda$) can still be described by Eq. (1) except that the persistence length l_p is now replaced with Γ^R.

In Fig. 4, we plot both $\Gamma^K(p)$ (high-tension regime) and $\Gamma^R(p)$ (low-tension regime) as functions of cisplatin occupancy. Recollecting that in the kink model, the distance between kinks is $2S$; therefore $p=a/2S$ in $\Gamma^K(p)$. Note that Γ^K is always smaller than Γ^R at any p. The difference in the effective persistence length between the two regimes is more pronounced as the cisplatin occupancy increases.

C. Analysis of experimental data

A DNA molecule was attached to a magnetic bead and introduced into the magnetic tweezers setup. With a bead of 1 μm size, we can apply up to 6 pN. Before adding cisplatin, the DNA molecule is held by a maximum force of around 6 pN. Then cisplatin at the concentration of 1000 μg/ml (3.3 mM) in salt solution is added to the sample chamber. During the incubation time, DNA extension decreases under constant tension. After a typical incubation time (ca. 30 min), excess cisplatin is washed out and the elastic property of cisplatin-bound DNA was obtained by measuring the force-extension curve. The measurements were performed for several different salt concentrations.

The extension $\langle x\rangle$ reflects the cisplatin occupancy. We compare the experimental results of force-extension measurement data of our DNA sample ($\sim$14.8 kb) with the theoretical estimates above. From the base sequence of the DNA, we obtained the information on a typical segment length between two consecutive G-G pairs. If the base sequence is "random," the probability of having a consecutive G-G is $p=1/16$. Indeed, the distance distribution between consecutive G-G pairs is fitted with an exponential distribution with the characteristic length of $16a$. Since kinks can also be associated with consecutive C-C's, complementary to G-G, a typical distance between possible cisplatin binding sites is $8a$.

The random-flight model is valid when tangent angles at kinks are not correlated with the direction of the external force ($\Lambda>l_p$). The elastic response in this regime is entropic and we fit the data with Eqs. (1) and (19). In the large-force regime ($\Lambda<l_p$), the stored length in kinks is pulled out and fluctuations are suppressed. The aligned-kink model applies in this regime. The force-extension relation was fitted with the following standard worm-like chain (WLC) model:

$$\frac{f}{k_BT}=\frac{1}{\Gamma(p)}\left\{\frac{1}{4}\left(1-\frac{x+b}{L}\right)^{-2}-\frac{1}{4}+\frac{x+b}{L}\right\}, \qquad (20)$$

where b is a fitting parameter reflecting the uncertainty on the attachment point of the DNA terminus on the bead. The effective persistence length $\Gamma(p)$ is Γ^K (Γ^R) in low-tension (high-tension) regime.

In Fig. 3, we present the experimental data of force-extension relation together with the fitting curves using Eq. (20) in both high- and low-tension regimes. All data from several batches can be consistently represented in Fig. 4. As seen below, the concentration of NaCl in the reaction buffer influences the cisplatin binding dramatically. The platination of DNA is far less efficient at high salt concentration
(>90 mM), while it is nearly saturated at low salt concentration (<10–20 mM). In Fig. 3(a), we show the force-extension curve of DNA incubated with cisplatin in 20 mM NaCl. The fitted effective persistence lengths are $\Gamma^K=9$ nm in the high-tension regime and $\Gamma^R=12.5$ nm in the low-tension regime. The crossover from the low- to high-tension regime occurs around $f\approx0.4$ pN, which is consistent with the condition $2\Lambda\approx l_p$. The corresponding cisplatin occupancy is $p^K(=a/S)\approx0.076$ [inferred from Eq. (15)] and $p^R\approx0.087$ [inferred from Eq. (19)]. This measurement was performed at the cisplatin occupancy which is about 2/3 of the theoretical saturation value where our previous assumption of noninteracting kinks is unlikely to be accurate even under the largest available pulling force. The experimental data for [NaCl]=60 mM (+ in Fig. 4) are shown in Fig. 3(b) together

with their theoretical fits. For both regimes, we obtain $\Gamma^K = 20$ nm and $\Gamma^R = 25$ nm, which yield $p^K = 0.032$ and $p^R = 0.029$, respectively. These values are in good agreement and the estimate of a true cisplatin occupancy would be $p = 0.031 \pm 0.002$. At [NaCl]=90 mM (∗ in Fig. 4), the effective persistence lengths in the two different regimes (Γ^R and Γ^K) converge to $\Gamma^K \simeq \Gamma^R = 40$ nm and the cisplatin occupancy is shown to be reduced ($p = 0.0073$). At an even lower platination, as is the case for [NaCl]=180 mM [Fig. 3(c); □ in Fig. 4], both persistence lengths (≈48 nm) are basically the same as that of bare DNA.

Under various experimental conditions, the persistence lengths deduced from the experimental data are presented in Fig. 4 and used to determine the degree of platination likewise. We mark all data sets of deduced effective persistence lengths and the corresponding platination degrees ($\Gamma^{K,R}, p^{K,R}$) on the theoretical curves. The cisplatin occupancies p^K and p^R obtained from the high- and low-tension regimes of the same force-extension curve are indicated as the y coordinates of identical symbols. Ideally, the two identical symbols should align horizontally, as p should not be different for both regimes. The discrepancy indicates the precision of determining cisplatin occupancy with this method. The theoretical maximum of p (=1/8) is marked as a double dotted line. Formally, one can reach the decoupled kink regime by applying a corresponding large force. However, our experiment only allows for moderate tension; the aligned-kink model is unlikely to be accurate when cisplatin occupancy is high. The highest occupancy where kinks can be efficiently decoupled in our experiment (maximum tension of 6 pN) is indicated in Fig. 4 as a dotted line. At the high kink density, kinks remain somewhat correlated even at 6 pN and, consequently, the accuracy of Γ_K is compromised there.

Figure 4 includes data from two different cisplatin batches. It should however be noted that cisplatin activity decreases upon aging. To correlate the degree of platination to the cisplatin concentration or to the salt concentration at fixed cisplatin concentration, only the data from the same batch could be compared and the experiments should be completed within a limited period of time (say, within 1 or 2 weeks).

III. DISCUSSION

In this study, we considered the elasticity of a single cisplatin-DNA adduct which includes quenched sequence of kinks with a fixed angle. Double-bound cisplatin is strongly linked to the DNA and is unlikely to be exchanged with the buffer or to travel along the sequence during measurements. We provided theoretical models for two limiting regimes of tension: the linear regime (low extension) and the uncorrelated kink regime (high extension).

The elastic response of platinated DNA in the linear regime clearly shows strengthening compared to that of bare DNA. This corresponds, according to the fluctuation dissipation theorem, to a reduction in the average end-to-end distance squared. It is possible to attribute the shrinking and strengthening upon platination to a decrease in the effective persistence length. A random-flight model does account for this effect. At high tension, the elasticity of the adduct shows even more strengthened behavior than the extrapolated WLC behavior from the low-force regime [see Figs. 3(a) and 3(b)]. In the high-tension regime, yet far below the B-S or melting transition, we propose a model for uncoupled kinks distributed on an almost straight filament. The elastic response originates from two effects: (i) tension-dependent reduction in the size of the deformed region around a kink (the very kink angle being imposed) and (ii) ironing-out of thermal fluctuations.

In both regimes, only the density of kinks is the relevant parameter for the adduct elasticity. Whenever these two regimes are within experimental reach, a fit involving two different persistence lengths allows us to extract the degree of platination (density of kinks) independently from both regimes and the consistency required for the degree of platination can be checked. This method has several limitations at high kink density (close to saturation). In our experiment the maximum force is not enough to decouple the kinks at the saturation level. The continuum model of DNA we adopt here may not be sufficiently accurate either (kinks being too close to each other). Notwithstanding the limitations, we were able to consistently measure the degree of platination over a large range.

It turns out that the salt concentration influences the binding efficiency of cisplatin significantly. Sodium chloride present in the reaction bath dramatically suppresses the observed strengthening, implying little or no cisplatin binding in the salt concentrations of $\sim 0.1M$. At such high salt concentration, excess Cl^- ions shift chemical equilibrium toward favoring the neutral form. The neutral form of cisplatin is unable to bind to DNA *in vitro*. *In vivo* [4] the neutral form (in contrast to the charged ones) can passively diffuse through the cell membrane. Inside the cell the chloride concentration is much lower (4–10 mM) and cisplatin hydrolyzes to the active charged form that binds to DNA. Besides the passive diffusion through the membrane, active processes are also involved [4]. Note that other anions besides Cl^-, e.g., carbonates and phosphates (present in the cell), can also suppress the mechanical signature of platination, for example, by favoring monoadducts. Moreover, some of those anions are known to be platinum ligands and to interfere with the platination of DNA. Nevertheless, the platination of chromosomal DNA is known to be quite efficient [4]. As a passive anion (not acting as a ligand for platinum, e.g., NO_3^-) should have little effect on binding, it would be interesting to quantify the sensitivity of binding to the chemical nature of added anions. In a marked contrast, small passive divalent counterions (cations) could strongly deplete cisplatin close to DNA. In addition, higher-valency cations (tri- and tetravalent) are known to lead to DNA collapse, while divalent cations should lead to moderate shrinking in a few millimolars range [30]. Some cations, such as Mg^{2+} (or Ca^{2+}), have an additional specific (nonelectrostatic) affinity for DNA [30,31] mainly through hydrogen bonding to the hydration shell of DNA. Experimental data on salt effects will be reported in detail elsewhere [32].

We provided a theoretical model for the elasticity of cisplatin-bound DNA whose backbone is deformed due to the formation of permanent kinks. By applying our theory to

the force-extension data obtained with the magnetic tweezers technique, we consistently predicted the degree of platination. It was also possible to quantify the influence of salt (here mainly sodium chloride) on platination. Future extensions of this work include testing of platination under conditions close to a physiological one.

ACKNOWLEDGMENTS

The authors acknowledge P. Baxter (ICS, Strasbourg), S. Harlepp, P. Hebraud, J. P. Munch (IPCMS, Strasbourg), B. Geny (ULP, Strasbourg), and I. Kulic (Harvard) for enjoyable discussions. N.-K.L. acknowledges financial support from the Korea Science Engineering Foundation (KOSEF) grant funded by the Korean government (MOSEF) (Grant No. R01-2007-000-10854-0). A.J. and N.-K.L benefited from the KOSEF/CNRS exchange program. S.O. acknowledges support from ACS Petroleum Research Fund (PRF) Grant No. 43923-AC7. This work was also supported in part by a Korea Research Foundation (KRF) grant funded by the Korean government (MOEHRD, Grant No. KRF-2007-C00129) and by the Seoul R&BD Program (S.-C. H.).

[1] B. Rosenberg, L. VanCamp, and T. Krigas, Nature (London) **205**, 698 (1965).
[2] H. C. Harder and B. Rosenberg, Int. J. Cancer **6**, 207 (1970).
[3] Y. Sedletska, M.-J. Giraud-Panis, and J.-M. Malinge, Curr. Med. Chem. **5**, 251 (2005).
[4] Y. Jung and S. J. Lippard, Chem. Rev. (Washington, D.C.) **107**, 1387 (2007).
[5] N. Poklar, D. Pilch, S. Lippard, E. Redding, S. Dunham, and K. Breslauer, Proc. Natl. Acad. Sci. U.S.A. **93**, 7606 (1996).
[6] S. Sherman and S. Lippard, Chem. Rev. (Washington, D.C.) **87**, 1153 (1987).
[7] D. Yang, S. van Boom, J. Reedijk, J. van Boom, and H. A.-J. Wang, Biochemistry **34**, 12912 (1995).
[8] J. den Hartog, C. Altona, J. van Boom, G. van der Marel, C. Haasnoot, and J. Reedijk, J. Biomol. Struct. Dyn. **2**, 1137 (1985).
[9] F. Herman, J. Kozelka, V. Stoven, E. Guittet, J.-P. Girault, T. Huynh-Dinh, J. Igolen, J.-Y. Lallemand, and J.-C. Chottard, Eur. J. Biochem. **194**, 119 (1990).
[10] P. M. Takahara, A. C. Rosenzweig, C. A. Frederick, and S. J. Lippard, Nature (London) **377**, 649 (1995).
[11] A. Gelasco and S. J. Lippard, Biochemistry **37**, 9230 (1998).
[12] S. F. Bellon, J. H. Coleman, and S. J. Lippard, Biochemistry **30**, 8026 (1991).
[13] S. F. Bellon and S. J. Lippard, Biophys. Chem. **35**, 179 (1990).
[14] J.-S. Park, B. Jeong, K.-J. Lee, S.-C. Hong, J.-Y. Hyon, and S.-M. Hong, J. Korean Phys. Soc. **49**, 963 (2006).
[15] N.-K. Lee, J.-S. Park, A. Johner, S. Obukhov, J.-Y. Hyon, K.-J. Lee, and S.-C. Hong, Phys. Rev. Lett. **101**, 248101 (2008).
[16] Z. Bryant, M. D. Stone, J. Gore, S. Smith, N. Cozzarelli, and C. Bustamante, Nature (London) **424**, 338 (2003).
[17] S. B. Smith, L. Finzi, and C. Bustamante, Science **258**, 1122 (1992).
[18] S. Harlepp, T. Marchal, J. Robert, J. F. Leger, A. Xayaphoummine, H. Isambert, and D. Chatenay, Eur. Phys. J. E **12**, 605 (2003).
[19] R. Krautbauer, H. Klausen-Schaumann, and H. E. Gaub, Angew. Chem., Int. Ed. **39**, 3912 (2000).
[20] J. Li, P. C. Nelson, and M. D. Betterton, Macromolecules **39**, 8816 (2006).
[21] P. A. Wiggins, R. Phillips, and P. C. Nelson, Phys. Rev. E **71**, 021909 (2005).
[22] Y. O. Popov and A. V. Tkachenko, Phys. Rev. E **71**, 051905 (2005).
[23] I. M. Kulic, H. Mohrbach, V. Lobaskin, R. Thaokar, and H. Schiessel, Phys. Rev. E **72**, 041905 (2005).
[24] In adopting this model we are going to neglect the small unwinding at kinks mentioned previously.
[25] N.-K. Lee and D. Thirumalai, Biophys. J. **86**, 2641 (2004).
[26] J. Marko and E. Siggia, Macromolecules **28**, 8759 (1995).
[27] E. Farge and A. C. Maggs, Macromolecules **26**, 5041 (1993).
[28] T. R. Strick, J.-F. Allemand, D. Bensimon, A. Bensimon, and V. Croquette, Science **271**, 1835 (1996).
[29] N.-K. Lee, A. Johner, and S.-C. Hong, Eur. Phys. J. E **24**, 229 (2007).
[30] N. V. Hud and M. Polak, Curr. Opin. Struct. Biol. **11**, 293 (2001).
[31] T. Chiu and R. Dickerson, J. Mol. Biol. **301**, 915 (2000).
[32] J.-S. Park, J.-Y. Hyon, N.-K. Lee, A. Johner, K.-J. Lee, and S.-C. Hong (unpublished).